Advanced Composite Materials
Publication details, including instructions for authors and subscription information:
http://www.tandfonline.com/loi/tacm20

Resin Impregnation Behavior in Processing of Unidirectional Carbon Fiber Reinforced Thermoplastic Composites

Satoshi Kobayashi [a] & Atsushi Tanaka [a]
[a] Graduate School of Science and Engineering, Faculty of Mechanical Engineering, Tokyo Metropolitan University, 1-1 Minami-Osawa, Hachioji, Tokyo 192-0397, Japan
Version of record first published: 17 Jul 2012.

To cite this article: Satoshi Kobayashi & Atsushi Tanaka (2012): Resin Impregnation Behavior in Processing of Unidirectional Carbon Fiber Reinforced Thermoplastic Composites, Advanced Composite Materials, 21:1, 91-102

To link to this article: http://dx.doi.org/10.1163/156855112X629559

///VSP///

Advanced Composite Materials 21 (2012) 91–102

ADVANCED COMPOSITE MATERIALS
brill.nl/acm

Resin Impregnation Behavior in Processing of Unidirectional Carbon Fiber Reinforced Thermoplastic Composites

Satoshi Kobayashi * **and Atsushi Tanaka**

Graduate School of Science and Engineering, Faculty of Mechanical Engineering, Tokyo Metropolitan University, 1-1 Minami-Osawa, Hachioji, Tokyo 192-0397, Japan

Received 4 August 2011; accepted 4 January 2012

Abstract

In order to fabricate composite components more rapidly, a micro-braiding technique has been proposed and investigated. In the present study, a simple model is proposed to predict resin impregnation process based on Darcy's law and the continuity equation. Bending modulus was also modeled considering the difference between tensile and compressive moduli of a carbon fiber and resin impregnation. To confirm the validity of the models, carbon fiber reinforced polypropylene composites were molded under various molding conditions. Cross-sectional observation results indicated that, by using the model proposed, it was possible to predict resin impregnation. Four-point bending tests were also conducted on the composites. It is confirmed that bending moduli were well predicted based on the proposed model.

Keywords

Continuous fiber, thermoplastics, resin impregnation, Darcy's law, carbon fiber, polypropylene

1. Introduction

Fiber reinforced plastics (FRP) are superior in processability, specific strength and fatigue life so that they have been used in the various fields of engineering, such as aerospace, automobile, marine, construction, etc. Currently, the matrix material used for FRP is thermoset plastics. However, thermoset plastics are more brittle and have lower impact resistance compared with thermoplastics in many cases. In addition, thermoset plastics require much processing time, because of the polymerization involved. On the other hand, a state variation is used in thermoplastics processing so that much reduced process time is achieved. Moreover, prepregs as intermediate materials for thermoset FRP, whose resins are B-stage state, should be stored in a cold dark place and their properties degrade with storage period. Storage

* To whom correspondence should be addressed. E-mail: koba@tmu.ac.jp
Edited by the JSCM

DOI:10.1163/156855112X629540

of intermediate materials of FRP with thermoplastics is easy and semi-permanent, because polymerization has finished. Thermoplastic FRP is also superior in recyclability, because the matrix can be made molten by heating and is separated from FRP.

Although thermoplastics have many merits as mentioned above, the viscosity of molten plastics is much larger, which results in lower impregnation in fiber yarns. In order to improve the impregnation of thermoplastics, many methods have been developed. Film stacking [1], powder impregnation [2] and commingled yarn [3] methods are taken as examples. In the film stacking method, matrix polymer films and reinforcing fabrics are alternately interlaced and then hot pressed. The powder impregnation method consists of fabrication of intermediate materials where reinforcing fiber yarns are combined with polymer powder. The commingled yarn method also utilizes intermediate materials where reinforcing and matrix fibers are evenly mixed as one yarn. These methods can improve the impregnation. However, there are also some problems. For example, the film stacking method may be applicable in the case of a polymer of low viscosity. For the powder impregnation method, it is difficult to handle the constituent materials since the polymer powder can be easily dislodged from the reinforcing filaments. In the commingled yarn method, the reinforcing fibers are easily damaged during the commingling process and a homogeneous distribution of reinforcement is expected.

Recently, the micro-braiding technique has been developed to solve these problems [4, 5]. In this method, matrix fiber yarns are braided around reinforcing fiber yarns with a traditional braiding technique and a micro-braided yarn as an intermediate material is obtained, as shown in Fig. 1. In a micro-braided yarn, the reinforcing fiber yarn contact with matrix fiber yarns is evenly distributed and higher impregnation is expected.

As stated above, the processability of thermoplastic FRP has been improved experimentally, while an analytical method to predict resin impregnation process is important to optimize a process condition. Analytical methods based on Darcy's law have been developed for the impregnation during vacuum assisted resin transfer molding using thermoset plastics [6]. However, few studies are available for the prediction of thermoplastics impregnation with a micro-braiding technique.

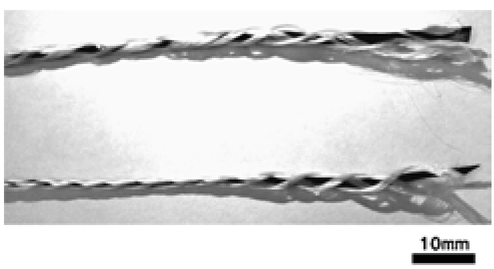

Figure 1. Micro-braided yarn.

In the present study, carbon fiber reinforced polypropylene composites were molded with a micro-braiding technique to investigate impregnation of thermoplastics in reinforcing fiber yarns. Moldings were conducted using micro-braided yarns under various molding conditions to clarify the relation between resin impregnation and molding condition, and between resin impregnation and a mechanical property.

2. Analyses

2.1. Impregnation

The prediction of the time necessity for the complete impregnation is important to determine the optimum molding condition and for the material design. Therefore, we derive the impregnation time based on Darcy's law for an incompressible fluid through a porous medium. Here, a coordinate as shown in Fig. 2 is assumed.

For the phenomenon of an incompressible fluid flow through a porous medium in z direction, a following equation is obtained according to Darcy's law,

$$u = -\frac{k}{\mu} \cdot \frac{\partial P}{\partial z}, \tag{1}$$

where u is the fluid velocity, μ is the viscosity of the fluid, $\frac{\partial P}{\partial z}$ is the pressure gradient and k is the permeability. From the equation of continuity,

$$\nabla \cdot \mathbf{u} = 0. \tag{2}$$

Equation (2) is expressed in a cylindrical coordinate system as

$$\frac{\partial u_x}{\partial x} + \frac{1}{r}\frac{\partial}{\partial r}(r u_r) + \frac{1}{r}\frac{\partial u_\theta}{\partial \theta} = 0. \tag{3}$$

In order to predict the impregnation time, the phenomenon of the uniform impregnation in the R direction in a fiber yarn with a radius of R_0 is considered. Assuming the velocity in the x direction is 0 and considering an axisymmetric condition, equation (3) is expressed as

$$\frac{1}{r}\frac{\partial}{\partial r}(r u_r) = 0. \tag{4}$$

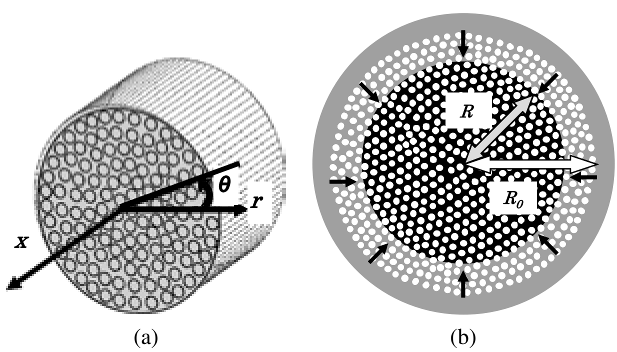

(a) (b)

Figure 2. Impregnation model. (a) Coordinate; (b) impregnation process.

From equations (4) and (1),

$$\frac{\partial P}{\partial r} = -\frac{\mu}{k} \cdot \frac{C_1}{r}. \tag{5}$$

Integrating equation (5) with respect to r,

$$P = -\frac{\mu}{k} \cdot C_1 \ln r + C_2 \tag{6}$$

is obtained, where C_1 and C_2 are constants.

As the boundary conditions:

1. $P = P_\mathrm{m}$ $(r = R_0)$ (P_m: molding pressure);
2. $P = P_0$ $(r = R)$ (R: distance from the center of the yarn to flow front of the resin, P_0: pressure atmosphere)

are used to determine C_1 and C_2. Then, equation (6) is expressed as

$$P = \frac{P_\mathrm{m}}{\ln(R_0/R)} \ln r - \frac{P_\mathrm{m}}{\ln(R_0/R)} \ln R = \frac{P_\mathrm{m}}{\ln(R_0/R)} \ln\left(\frac{r}{R}\right). \tag{7}$$

From equation (1),

$$u_r = -\frac{k}{\mu} \cdot \frac{\partial P}{\partial r} = -\frac{k}{\mu} \cdot \frac{\partial}{\partial r}\left\{\frac{P_\mathrm{m}}{\ln(R_0/R)} \ln\left(\frac{r}{R}\right)\right\} = -\frac{k}{\mu} \cdot \frac{P_\mathrm{m}}{\ln(R_0/R)} \cdot \frac{1}{r} \tag{8}$$

is obtained. Assuming the velocity $u_r = V$ at the flow front,

$$V = \frac{\mathrm{d}R}{\mathrm{d}\tau} = -\frac{k}{\mu} \cdot \frac{P_\mathrm{m}}{\ln(R_0/R)} \cdot \frac{1}{R} \tag{9}$$

is obtained. Rearranging equation (9) as

$$R \ln\left(\frac{R_0}{R}\right) \mathrm{d}R = -\frac{k}{\mu} P_\mathrm{m}\, \mathrm{d}\tau, \tag{10}$$

where τ is impregnation time. Integrating both members of equation (10) and applying the boundary condition $R = R_0$ at $\tau = 0$, following equation is obtained

$$\tau = -\frac{\mu}{k P_\mathrm{m}}\left\{\frac{R^2}{2} \ln\left(\frac{R_0}{R}\right) + \frac{R^2 - R_0^2}{4}\right\}. \tag{11}$$

Impregnation ratio, I, is defined as the ratio of the impregnation area to cross-sectional area of the yarn, as

$$I = \frac{\pi R_0^2 - \pi R^2}{\pi R_0^2} = 1 - \left(\frac{R}{R_0}\right)^2. \tag{12}$$

In the present study, τ is defined as the pressurizing duration from the beginning of the pressurizing to the beginning of the cooling (pressure is released as 0) and experimental results of the relation between I and τ are compared with the theoretical values. In experiments, I is not 0 at $\tau = 0$ because of the weight of the die and the capillary action during cooling. In order to fit the analytical values to the experimental data, the distance of the flow front, $R = R_0'$ ($R_0' < R_0$), is obtained based on the experimental value at $\tau = 0$. In experiments, let $I = I_0$ at $\tau = 0$, then

$$I_0 = 1 - \left(\frac{R_0'}{R_0}\right)^2. \tag{13}$$

From equation (13),

$$R_0' = R_0\sqrt{1 - I_0}. \tag{14}$$

In integrating equation (10), assuming the boundary condition as $R = R_0'$ at $\tau = 0$,

$$\tau = -\frac{\mu}{kP_\mathrm{m}}\left[\frac{R^2}{2}\ln\left(\frac{R_0}{R}\right) + \frac{R^2 - R_0^2(1 - I_0)\{1 - \ln(1 - I_0)\}}{4}\right]. \tag{15}$$

Substituting equation (12) into equation (15) and rearranging as

$$\tau = -\frac{\mu R_0^2}{4kP_\mathrm{m}}[(1 - I)(1 - \ln(1 - I)) - (1 - I_0)(1 - \ln(1 - I_0))]. \tag{16}$$

Equation (16) denotes the relation between impregnation ratio and time.

2.2. Bending Modulus

In the present study, 4-point bending tests were conducted as mentioned below and bending moduli were measured as the ratio of nominal bending stress to strain at the compressive surface. In this section, bending modulus is predicted analytically considering impregnation. Here, the following are assumed:

1. Carbon fibers in unimpregnated region can sustain the tensile loading, but cannot sustain the compressive loading.
2. $E_\mathrm{m} \ll E_\mathrm{f}$ so that $E_\mathrm{m} \approx 0$.
3. From 2, modulus of the composite is $v_\mathrm{f}E_\mathrm{f}$, where v_f is the fiber volume fraction.

Generally, compressive and tensile moduli (E_fc and E_ft, respectively) of a carbon fiber are different from each other. Thus, the following ratio is defined,

$$\beta = E_\mathrm{fc}/E_\mathrm{ft} \tag{17}$$

and α is defined as

$$\alpha = I \cdot \beta. \tag{18}$$

As shown in Fig. 3, the location of neutral plane t_n for the specimen with width, b, and thickness, t_0, is expressed as

$$t_\mathrm{n} = \frac{\int_0^{t_\mathrm{m}} yb\,\mathrm{d}y + \alpha\int_{t_\mathrm{n}}^{t_0} yb\,\mathrm{d}y}{bt_\mathrm{n} + \alpha b(t_0 - t_\mathrm{n})} \tag{19}$$

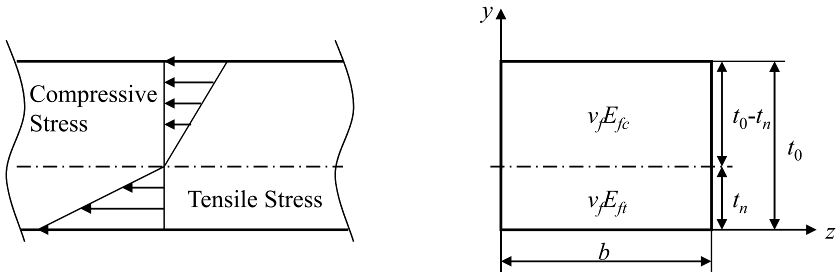

Figure 3. Coordinate for a beam in section.

and solving for t_{n},

$$t_{\mathrm{n}} = \frac{-\alpha + \sqrt{\alpha}}{1-\alpha} t_0 = \frac{\sqrt{\alpha}}{1+\sqrt{\alpha}} t_0. \tag{20}$$

Bending moment at the center of the specimen under 4-point bending with each loading distance, l, is

$$M = \frac{Fl}{2}. \tag{21}$$

Redefining the origin of y axis at the neutral plane, the bending moment is also expressed as

$$M = \int \sigma y \,\mathrm{d}A = \int_{-t_{\mathrm{n}}}^{t_0 - t_{\mathrm{n}}} \sigma y b \,\mathrm{d}y. \tag{22}$$

Assuming a radius of curvature of the composite as ρ, stress σ is

$$\sigma = E\varepsilon = E\frac{y}{\rho}. \tag{23}$$

From equations (20), (22) and (23),

$$\begin{aligned} M &= \int_{-t_{\mathrm{n}}}^{t_0 - t_{\mathrm{n}}} \frac{E}{\rho} y^2 b \,\mathrm{d}y = \frac{v_{\mathrm{f}} E_{\mathrm{f}}}{\rho} \int_{-t_{\mathrm{n}}}^{0} y^2 b \,\mathrm{d}y + \frac{\alpha v_{\mathrm{f}} E_{\mathrm{f}}}{\rho} \int_{0}^{t_0 - t_{\mathrm{n}}} y^2 b \,\mathrm{d}y \\ &= \frac{\alpha b v_{\mathrm{f}} E_{\mathrm{f}} t_0^3}{3\rho(1+\sqrt{\alpha})^2}, \end{aligned} \tag{24}$$

where compressive strain outermost ε_{c} is

$$\varepsilon_{\mathrm{c}} = \frac{t_0 - t_{\mathrm{n}}}{\rho}. \tag{25}$$

From equations (20), (21), (24) and (25), ε_{c} is obtained as

$$\varepsilon_{\mathrm{c}} = \frac{t_0}{\rho(1+\sqrt{\alpha})} = \frac{3Fl(1+\sqrt{\alpha})}{2\alpha b v_{\mathrm{f}} E_{\mathrm{f}} t_0^2}. \tag{26}$$

Since nominal bending stress is calculated as

$$\sigma = \frac{3Fl}{bt_0^2} \tag{27}$$

bending modulus E_b is expressed as

$$E_\mathrm{b} = \frac{\sigma}{\varepsilon_\mathrm{c}} = \frac{3Fl}{bt_0^2} \cdot \frac{2\alpha b v_\mathrm{f} E_\mathrm{f} t_0^2}{3Fl(1+\sqrt{\alpha})} = \frac{2\alpha v_\mathrm{f} E_\mathrm{f}}{1+\sqrt{\alpha}}. \tag{28}$$

3. Experimental

3.1. Micro-Braiding Method

Micro-braided yarn (MBY) was fabricated with a medium-class braider (Kokubun Limited Co.). As shown in Fig. 4, a reinforcing fiber yarn was located at the center of the braider and matrix fiber yarns were braided around the reinforcing fiber yarn. In the present study, one carbon fiber yarn of TR50S-6L (6000 filaments, 400 tex, Mitsubishi Rayon Co.) was used as a reinforcement. As the matrix, 4 yarns of polypropylene 760T120-20S (760 tex, MRC Pylene Co.) were selected.

3.2. Compression Molding

MBY was hot-pressed into the rectangular specimens. At first, MBY was wound on the metallic frame 15 times per 10 mm. MBY wound on the frame was placed on the preheated mold die with a demold treatment and was hot-pressed. Hot press system used was IMC-1837 (Imoto Co.). In the present study, molding pressure, temperature and time were defined as the pressure on the molded pieces, the temperature of the heating platens and the duration where pressure and temperature were kept, respectively. Molding condition conducted in this study is shown in Table 1. After keeping the molding pressure and the temperature for a given molding time, pressure was released and the molding die was cooled by a water flow in the cooling pipes through the heating platens to less than 50°C. For molding time of 0 min, it is noted that the mold die was pressed to the molding pressure and pressure was released immediately once reaching the molding pressure. Two specimens with 10 mm width and 200 mm length were obtained in one molding (see Fig. 5).

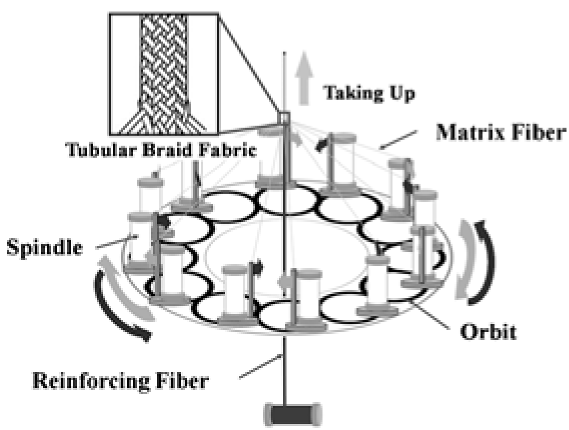

Figure 4. Braiding machine.

Table 1.
Molding conditions

Temperature (°C)	Pressure (MPa)	Holding time (min)
200, 220	8	0–10 (every 1 min)
	12	0–5 (every 1 min)

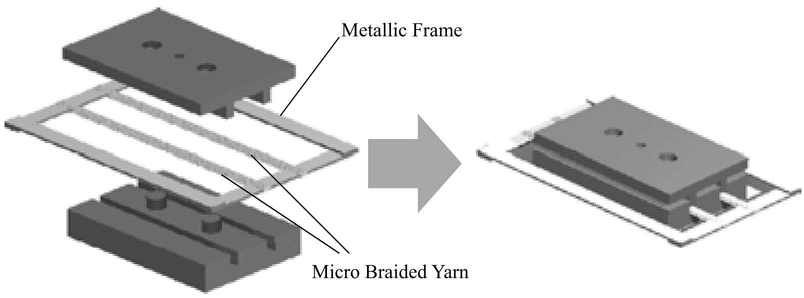

Figure 5. Micro-braided yarn set to a pair of molds.

3.3. Cross-Sectional Observation

In order to measure the impregnation ratio, cross-sectional observations were conducted at the center of the specimens molded at each condition. After the molded pieces were embedded in epoxy resin and resin was cured, the cross-section was polished using #180–2000 emery papers and was finished by buffing with aluminum slurry. Then, the polished surface was observed using a video microscope and digital images obtained were converted to bitmap files. Impregnation ratio was calculated as the ratio of the number of pixels in impregnation region to that of yarn region, including cross-sectional area of fibers.

3.4. Four-Point Bending Tests

In order to characterize the mechanical properties of the molded pieces, 4-point bending tests were conducted. The molded piece with 10 mm width was cut to 100 mm length using a diamond saw. A strain gauge (5 mm gauge length) was glued on the compressive surface in bending. The tests were conducted with a universal testing machine (AG-IS 50 kN, Shimadzu Co.) under cross-head speed of 1 mm/min. For the tests, a fixture with upper and lower spans of 24 and 72 mm and a load cell with capacity of 500 N were used. Bending stress was calculated using equation (27). Strain was also measured from a strain gauge glued to the specimen. In the present study, since only an initial elastic property was discussed, a test was performed up to about 0.4% strain. Bending modulus was calculated as the initial linear slope of the bending stress–strain curve.

4. Experimental Results and Discussion

4.1. Impregnation

Figures 6 and 7 show the enlargement images of cross-section for the molded pieces at molding temperature of 8 MPa and molding temperature of 200 and 220°C, re-

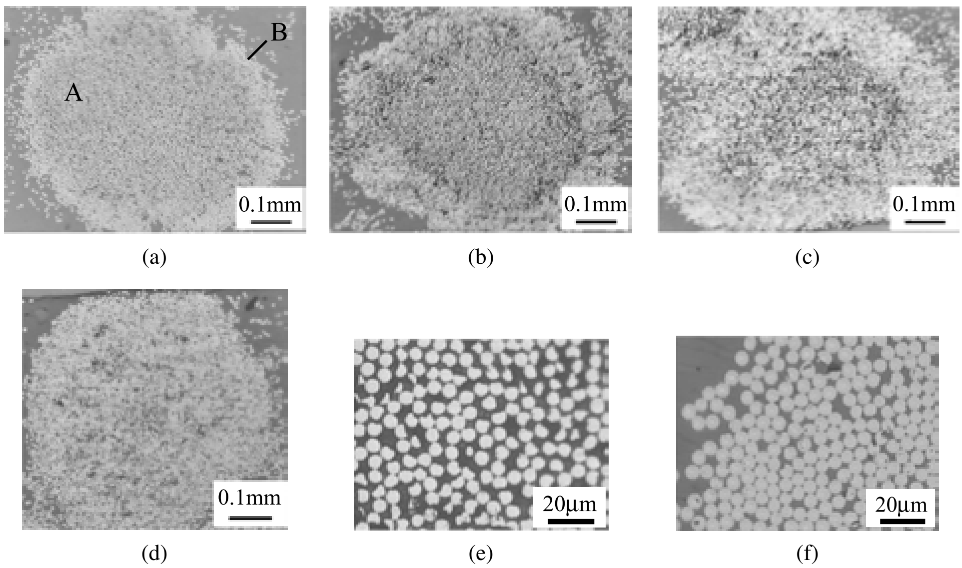

Figure 6. Cross-sectional photographs of CF/PP composites (200°C, 8 MPa). (a) 1 min. (b) 3 min. (c) 5 min. (d) 10 min. (e) A in (a) (not impregnated). (f) B in (a) (impregnated).

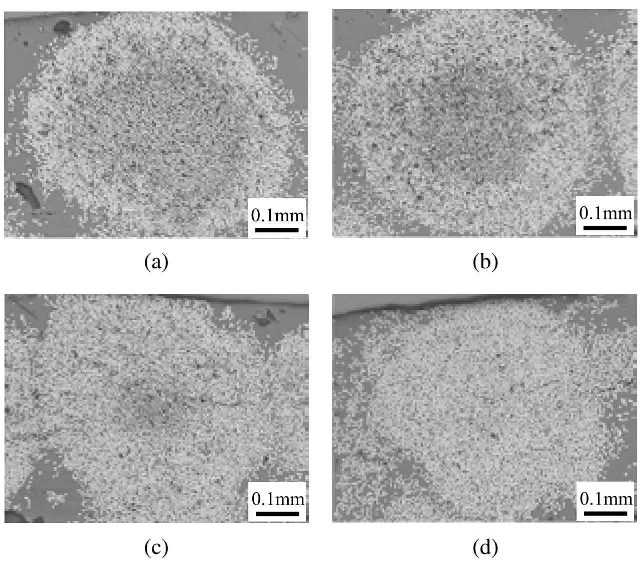

Figure 7. Cross-sectional photographs of CF/PP composites (220°C, 8 MPa). (a) 1 min. (b) 3 min. (c) 5 min. (d) 10 min.

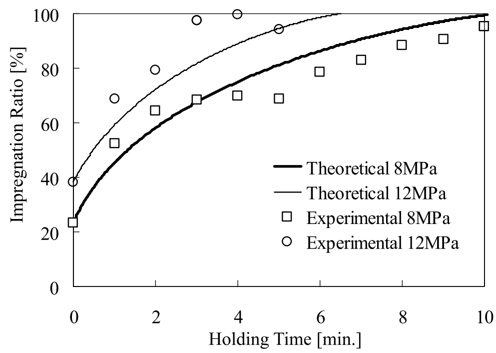

Figure 8. Impregnation ratio as a function of holding time (200°C).

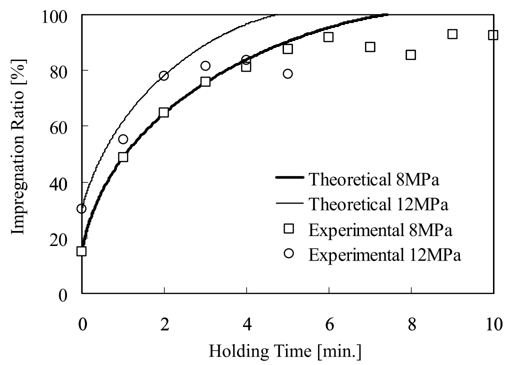

Figure 9. Impregnation ratio as a function of holding time (220°C).

spectively. Impregnation ratios measured from them are also shown in Figs 8 and 9, respectively. Figures 8 and 9 include the analytical predictions made by curve fitting equation (16) to the experimental results with variation in the value of μ/k. P_{m} used was the molding pressure. The yarn radius was measured from the micrograph as $R_0 = 0.6$ mm. In order to fit an equation (16) to the experimental results, the values of μ/k were selected as 5.7×10^{16} kg/s $\cdot$ m^3 for 200°C and 4.0×10^{16} kg/s $\cdot$ m^3 for 220°C. As shown in Figs 8 and 9, fair agreements for impregnation between experiments and analyses were obtained, regardless of molding pressure. Thus, at the same molding temperature, once the μ/k value is determined for a given pressure, the prediction for arbitrary pressure is available. Some contradictions between experiments and analyses are due to the assumption of constant fiber volume fraction. The effect of fiber volume fraction variation will be considered in our future analysis.

μ/k values decreased with molding temperature. This is attributed to the decrease in viscosity of polypropylene. From [7], the viscosities of polypropylene are 4260 Pa $\cdot$ s at 200°C and 3100 Pa $\cdot$ s at 220°C. With these values, k values are calculated as 747×10^{-16} m^2 for 200°C and 775×10^{-16} m^2 for 220°C. Considering the scatter in the measurements, this result suggests that k is a constant for a yarn and is independent of molding condition. In other words, when viscosity is known as a function of temperature, once k is determined in a preliminary experiment, it is possible to predict the impregnation behavior at any molding conditions. On the other hand, analytical prediction overestimates the impregnation for longer molding time at 220°C. The possible reasons are pyrolysis of resin and/or fiber stuck in the equipment. In the future work, these effects should be considered in the analysis.

4.2. Mechanical Property

Figures 10 and 11 show the relation between bending modulus of the composite and molding time at 200 and 220°C, respectively. Bending modulus increased with increasing molding time and had the same tendency with the impregnation ratio as shown in Figs 8 and 9. Bending moduli considering impregnation ratio calculated using an equation (28) are also shown in Figs 10 and 11. In the calculation, impregnation ratios as a function of molding time used were analytical values in Figs 8 and 9. The ratio β used was for a PAN-based medium modulus carbon fiber [8] and E_{ft} was 240 GPa from a catalog. The v_{f} value used was 43% which corresponded with a fiber volume fraction in MBY. Theoretical predictions are in good agreement

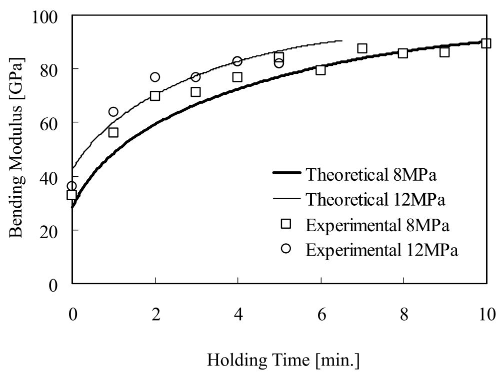

Figure 10. Bending modulus as a function of holding time (200°C).

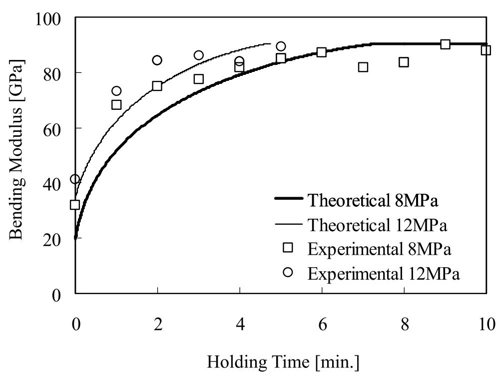

Figure 11. Bending modulus as a function of holding time (220°C).

with experimental results. From the results, once impregnation is determined, it is possible to predict the bending modulus. Moreover, impregnation ratio is roughly estimated by conducting a bending test on a specimen cut from a molded article.

5. Conclusion

The relation between resin impregnation and molding condition of continuous carbon fiber reinforced polypropylene fabricated using a micro-braiding technique was investigated. An analytical model for impregnation was derived based on Darcy's law. Comparisons between experiments and analyses indicated the effectiveness of the proposed model and that the permeability is independent from molding temperature, and therefore from the viscosity of the molten plastics. Bending modulus prediction considering impregnation ratio and the difference in tensile and compressive moduli of carbon fiber was proposed. It is clarified that this model well predicts the relation between bending modulus and molding time.

References

1. E. K. Gamstedt, L. A. Berglund and T. Peijs, Fatigue mechanism in unidirectional glass-fiber-reinforced polypropylene, *Compos. Sci. Technol.* **59**, 759–768 (1999).
2. A. Miller, C. Wei and A. G. Gibson, Manufacture of polyphenylene sulfide (PPS) matrix composites via the powder impregnation route, *Composites A* **27A**, 49–56 (1996).
3. L. Ye, K. Friedrich, J. Kästel and Y.-W. Mai, Consolidation of unidirectional CF/PEEK composites from commingled yarn prepreg, *Compos. Sci. Technol.* **54**, 349–358 (1995).
4. M. Sakaguchi, A. Nakai, H. Hamada and N. Takeda, The mechanical properties of unidirectional thermoplastic composites manufactured by a micro-braiding technique, *Compos. Sci. Technol.* **60**, 717–722 (2000).
5. K. Fujihara, Z.-M. Huang, S. Ramakrishna and H. Hamada, Influence of processing condition on bending property of continuous carbon fiber reinforced PEEK composites, *Compos. Sci. Technol.* **64**, 2525–2534 (2004).
6. P. B. Nedanov and S. G. Advani, A method to determine 3D permeability of fibrous reinforcements, *J. Compos. Mater.* **36**, 241–254 (2002).
7. D.-H. Han, J.-H. Jang, B.-G. Cho, B.-N. Kima and G.-S. Seo, Melt complex viscosity and molecular weight for homo-polypropylene modified by grafting bifunctional monomers under electron beam irradiation, *Polymer* **47**, 6592–6597 (2006).
8. N. Oya and D. J. Johnson, Longitudinal compressive behavior and microstructure of PAN-based carbon fibers, *Carbon* **39**, 635–645 (2001).